ATL-TILECAL-2000-006
28/02/2000

Studies of the optics response of Steel-plastic scintillator calorimeters for the ATLAS detector and checks of lights sources for their quality control[1]

Oscar Blanch Bigas
Universitat Autònoma de Barcelona
Departament de Física
Institut de Física d'Altes Energies
Edifici Cn E-08193 Bellaterra (Barcelona)

September 1999

[1] Treball de recerca de Tercer Cicle en Físiques

A tots aquells per qui he plorat.

ELS AGRAÏMENTS

Tot té un inici i el meu inici en el món de la Física d'Altes Energies el dec a l'Enrique Fernández. Ell em va donar l'oportunitat d'entrar a l'IFAE la qual cosa no només haig d'agrair sinó que a més ho vull fer.

Durant aquest dos anys he tingut la gran sort de treballar amb gairebé tots els sèniors de l'IFAE. És cert que per diverses raons no he pogut treballar amb cap d'ells el temp suficient com per aprendre'n ni una centèsima part del que tenen per ensenyar, però crec que no vaig gaire errat si dic que això tampoc ho hagués aconseguit si només hagués treballat amb un d'ells. En canvi tots m'han ensenyat coses molt importants que possiblement un sol no hagués pogut. Es diu que a la diversitat s'hi troba la força i crec que en aquest cas la dita és certa. Alguns d'ells han col·laborat directament en el treball que segueix a aquests agraïments com són el Manuel (qui a més ha realitzat el paper de director), la Martine i el Mokhtar. Altres no han tingut una col·laboració tant directa, però no per això deixa de ser important: Matteo, Lluís i George. I finalment també he interaccionat amb sèniors per feina que no té cap mena de relació amb el que està recopilat ens el cent i escaig fulls que segueixen aquest com és el cas del Manel. De tots ells n'admiro alguna cosa, però des del meu punt de vista allò que els caracteritza és: la capacitat de síntesi, la disposició, el detallisme, la curiositat, la confiança, la capacitat de treballar i la capacitat de generar idees, per ordre d'aparició, o no.

Ja sé que posar ara les persones que vull posar va en certa manera en contra de les tradicions. Però crec que és de justícia donar les gràcies ara i aquí a les persones de les que més coses he après sobre TILECAL i el Cs. Sense elles dues la realització d'aquest treball hagués estat infinitament més difícil i lenta. Elles són la Sílvia i la Irene. També és de justícia agrair l'ajut en el muntatge experimental del Mini-Mòdul del Sasha i el Jose.

Pel que fa a la resta de la gent que ha format o forma part de l'IFAE i que no pertanyen a l'espècie que anomenem estudiants puc dir ben poca cosa ja que no he tingut la oportunitat de treballar-hi. De totes maneres tampoc seria just deixar-los de banda i aquest paràgraf està dedicat a ells.

Finalment hem arribat a l'últim, però no per això menys important, grup de gent que forma l'IFAE. De fet per mi ells són l'autèntic IFAE i aquest grup no és altre que el dels estudiants. Hi ha alguns que ja han marxat: Aurelio, Imma i Gaelle. Altres ja hi eren quan vaig arribar, però encara no han marxat (ni ganes): Pilar, Eugeni, Gon, Hugo i Sílvia. També

existeixen aquells que van entrar més tard: David, Pepe, Javi, Dani i Thomas. I fins i tot alguns acaben d'entrar: Eva i Xavier. Ah!!! És veritat, també hi ha la subspècie dels enginyers: Edu, Eduard, Xavi, Juan Carles, Laia i Lluís. A tots vosaltres moltes gràcies per haver creat, i espero que mantenir, l'ambient que es respira dins aquestes quatre parets i que fins i tot sou capaços de transportar a l'exterior. Possiblement tots us mereixeu com a mínim unes línies i de fet hi ha algú que ja les ha tingut, però …amb l'esperança que ningú s'ho prengui malament només les dedicaré a aquells amb qui per A o per B hi he tingut més relació.

Començaré per la Imma, ella va ser la meva companya de despatx. Possiblement no vam estar compartint despatx en el millor moment per cap dels dos. Però tot i així quan arribava aquell instant en el qual ja no podies seguir treballant sempre la trobaves disposada a xerrar cinc minutets. Just el necessari per recarregar piles. A continuació et tocarà el rebre a tu, Hugo. Com vols que t'ho digui. Sempre és divertit veure les teves cares de sorpresa. Però aquestes línies te les has guanyat per ser tant amable amb mi i deixar-me ser-ho amb tu. I per últim, no pas per importància sinó per antiguitat, en aquest paràgraf apareixerà la Laia. Encara no entenc exactament com va començar tot, però des de que realment ens coneixem has acumulat infinitat de coses per agrair. Els teu mails sempre (o gairebé sempre) són un font d'alegria i diversió. I la capacitat per escoltar no té preu.

Per acabar amb aquells que he conegut gràcies a la física cal recordar la gent que em vaig trobar durant els meus anys de carrera: Roger, Jordi, Marc, Oriol, Roser, Martí, Jaume, Guillem … amb els quals encara mantinc alguna mena de contacte. I la gent que he trobat aquests dos últims anys: Santi, Farida, Roger, Lucía, Pablo, Núria, Aitor,… Tots ells han col·laborat de forma decisiva a que la física no sigui només la meva llicenciatura sinó també el meu millor passatemps.

Efectivament no tot a la vida és física (alguns diuen que la química és més important) i per tant també es mereixen un paràgraf tots aquells que m'han donat suport en els moments difícils i amb els que he gaudit de molts bons moments. Encara que la física els hi quedi ben lluny. No sé si mai ho llegireu, però sí! Estic parlant de vosaltres: Txell, Pau, Miki, Jordi ,… i el bàsquet. Sense ells tot hagués estat molt més dur.

I la meva família.

Òbviament tots els que em coneixeu mínimament sabeu que hi ha una persona que haig d'anomenar i que encara no ho he fet. La veritat és que ho he estat enrederint bàsicament perquè no sé què posar. Per una banda li dec tant i li haig d'agrair tantes coses que no sé per on començar i, el que és més important ja que aquest agraïments no poden ser quilomètrics,

no sé quan acabaria. A més la meva capacitat poètica, descriptiva, creativa o com li vulgueu dir no és suficient per dir amb poques paraules tot el que ella ha significat, significa i estic segur que seguirà significant per mi. Ni tant sols sé si ho podria dir amb moltes paraules. Per tant simplement et diré una cosa: moltíssimes gràcies per ser com ets, Mireia, i per la teva amistat.

MOLTÍSSIMES GRÀCIES A TOTS I FINS SEMPRE.

CONTENTS

1. INTRODUCTION

The LEP (Large Electron Positron collider) experimental program has confirmed the validity of the Standard Model up to energies of about 200 GeV. However, there are still questions to be answered in the Standard Model frame, such as the existence of the Higgs boson. Besides that, theories that go beyond the Standard Model predict the discovery of new physics at the TeV energy scale.

The LHC (Large Hadron Collider) is designed to reach this high energy region and it will be built at CERN using the current LEP tunnel. It will be a proton-proton collider, hence the synchrotron radiation that limits the energy in an electron-positron cicular collider such as LEP, will not be a significant problem. The collision energy will be about 14 TeV using magnetic fields of the order of 10 Tesla generated in superconductive magnets.

Since most of the physical questions to be answered involve interactions with very low cross section, not only a high energy but also the maximum possible luminosity is required. The LHC will reach luminosities of 10^{34} cm $^{-2}$ s^{-1} with interbunch crossing times of the order of 25 ns, which will result in more than 10^9 interactions per second.

ATLAS is one of the detectors designed to operate at the LHC and exploit its discovery potential. ATLAS will follow the usual model for collider detectors and will have several cylindrically symmetric concentric layers of detection elements. The hadron calorimeter component will be a steel-scintillator sampling calorimeter (TILECAL) and will play an important role by providing measurements of jet energies and directions as well as missing energy measurements.

During 1998 a full scale prototype module equipped almost as in the final ATLAS design (which will be referred to as B98), has been constructed and tested by exposing it to muon, pion, and electron beam at the CERN SPS. It has also undergone calibration using electronic charge injection, laser light pulses, and radiation from a ^{137}Cs source. The light yield of Barrel 98 as well as for previous prototypes built in 1996 and 1997 [1] showed some small irregularities that were not understood. A TILECAL prototype (which will be referred to as the Mini-Module) was built to find out which might have been the reason for them. The Mini-Module was also used to check if a LED would be suitable for the quality control (QC) during the production of TILECAL modules. The aim of this work is to show that the LED system satisfies the requirements for the TILECAL QC and to exploit the information that the data from this system

as well as from the Cs calibration system gives about the light yield of the calorimeter. Also, some MonteCarlo studies of disuniformities in the calorimeter, which would affect the energy resolution, will be made.

This work is organised as follows: in Chapter 2 general notions on electromagnetic and hadron calorimetry are given. In Chapter 3 the ATLAS detector is described, with emphasis on the Hadronic Tile Calorimeter. In Chapter 4 the calibration of the Tile Calorimeter detector is reviewed. In Chapter 5, the analysis of Cs calibration data from Ba98 is presented. The experimental set-up used for the Mini-Module studies and its data analysis are described in Chapter 6. In Chapter7, MonteCarlo simulation of how inhomogeneities in the optics would affect the muon energy resolution is shown. Finally, Chapter 8 gives the conclusions of this study.

2. CALORIMETRY

The principle of calorimetry is to perform the energy measurement of an incident particle by total absorption. In this chapter the basic processes for electromagnetic (e.m.) and hadronic showers will be described and some basic calorimeter concepts and limitations presented. Calorimeters will play an important role at high-energy machines; since in contrast to other detectors such as magnetic spectrometers, their intrinsic resolution improves with energy. In particular, at the LHC, calorimeters will be leading detectors in many measurements for the reconstruction of physics channels of prime interests.

2.1. What is a calorimeter?

Conceptually, a calorimeter is a block of matter which intercepts the primary particle, and is of sufficient thickness to cause it to interact and deposit all its energy inside the detector volume. At sufficiently high energy, this involves the formation of a cascade or "shower" of an increasing number of lower energy particles. Eventually, most of the incident energy is dissipated and appears in the form of heat. Some fraction (usually very small) of the deposited energy is detectable in the form of a more practical signal (e.g. scintillation light, Cherenkov light, or ionisation charge), which is proportional to the initial energy.

Calorimetric particle detectors can be divided in two types: homogeneous calorimeters and sampling calorimeters. In the first, the particles release all their energy in an active medium, which provides the measurable signal. In sampling calorimeters only a fraction of the energy is released in the active medium, which is interleaved between layers of passive absorber medium.

The key parameters that characterise calorimeters are the repeatability of response ("statistical" response) which determines the energy resolution of a detector, and the average response as a function of energy and type of particle. For electrons and photons only the e.m. interactions are important, providing the basis for e.m. calorimeters. Hadrons, however, are mostly absorbed through hadronic interactions, and therefore hadronic calorimeters are fundamentally different from e.m. calorimeters. Muons deposit energy predominantly through ionisation and excitation, leaving a distinctly different signature. Neutrinos, which interact only weakly, are indirectly detected through the absence of any energy deposit ("missing energy").

2.1.1 Main properties of calorimeters

i. They are sensitive to charged and neutral particles. They often provide the only practical method for measuring neutral particles, such as γ,n,π^o,K^0,ν.

ii. The energy measurement is based on the total absorption of the incident particle through a series of inelastic collisions degrading its energy. The average number $\langle N \rangle$ of secondary particles produced is proportional to the energy of the incident particle E. In principle, the uncertainty in the energy measurement is governed by statistical fluctuations in N, and hence the relative energy resolution σ/E improves as $1/\sqrt{\langle N \rangle} \sim E^{-1/2}$.

iii. The ideal calorimeter should contain the whole shower. Therefore, the depth of a calorimetric detector should match the scaling of the longitudinal shower profile, which is logarithmic with particle energy (see section 2.2). This can be compared to magnetic spectrometers, where the size scales with momentum as $p^{1/2}$, for a given relative momentum resolution $\Delta p/p$.

iv. They can be segmented to a very high degree, which allows a precise measurement of the direction of the incoming particles.

v. Their different response to electrons, muons, and hadrons can be exploited for particle identification.

vi. The energy information can be available on a relatively fast time scale, depending on the nature of the active medium. This feature is essential for online event selection ("triggering").

2.1.2 Readout systems for sampling calorimeters

i. *Light-collecting sampling calorimeters*

They are based on scintillating active media and the light is usually read by photomultipliers (PMTs) through wavelength-shifters (WLS) or scintillator plates individually coupled to a light guide. The use of WLS materials is often essential because the spectrum of emission of the scintillator does not overlap with the region of high quantum efficiency of the PMT. Scintillation light crosses an air gap and enters the WLS, where it is absorbed and subsequently re-emitted at longer wavelengths. A fraction of this wavelength-shifted light is then internally reflected to the light detector. Scintillating fibres have existed since the 50's but have been successfully used only in the last decade [2.1.]. This is mainly a consequence of the improvement in the quality of fibres in that time.

ii. *Charge collection readout.*

The ionisation charge produced by the passage of the charged particles of the shower may be collected from solids, liquids, or gases. Solids and liquids can only be used in an ionisation

chamber mode with no internal amplification. The best known and, to date, the only practical example is based on the use of liquid Argon. If gas is used as the active sampling medium, internal amplification using wire chambers is usually exploited.

2.2. Electromagnetic showers

The principal mechanisms by which particles that interact only electromagnetically lose their energy in matter include well-understood effects, which are governed by the laws of quantum electrodynamics. There are two high-energy (E≥100 MeV) e.m. energy loss mechanisms through which the e.m. cascade propagates. Electrons and positrons lose energy by radiation (bremsstrahlung, see figure 2.1), whereas photons produce electron-positron pairs (figure 2.2).

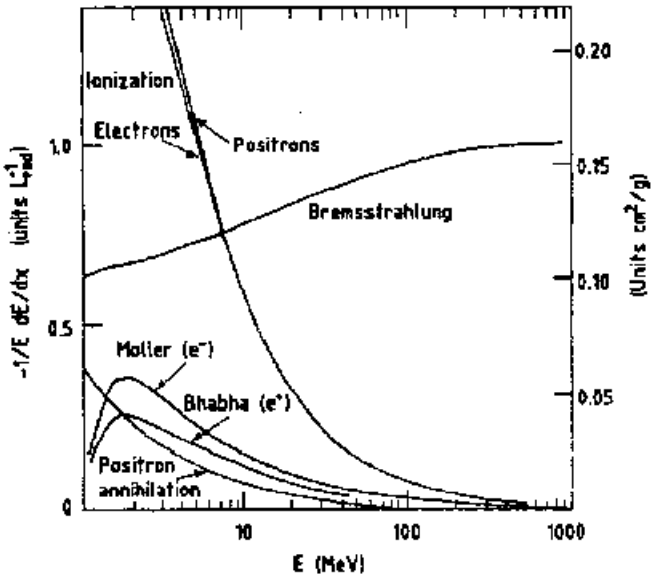

Fgure 2.1. Energy loss mechanisms for electrons and positrons.

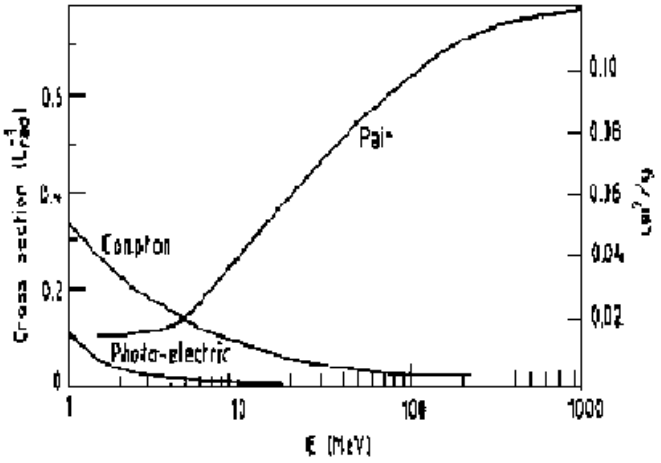

Figure 2.2. Photon cross section in lead as a function of photon energy.

Although the probabilities for these processes depend on energy, one can assume a constant cross section or constant mean free path between energy degrading collisions because the energy dependence is very small. This picture leads to a one-dimensional cascade model, as sketched in figure 2.3.

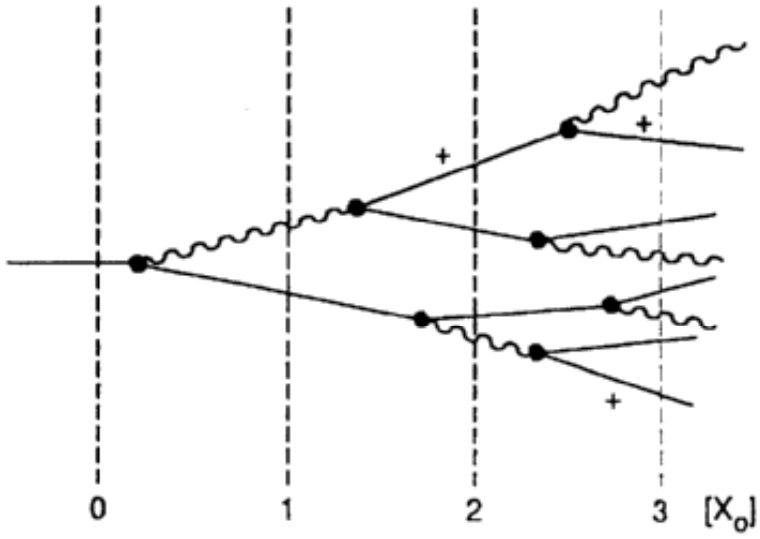

Figura 2.3. One-dimensional cascade model of the e.m. shower.

In order to discuss e.m. calorimetry independently of the material used, it is convenient to introduce two quantities [2.2.]:

- The critical energy, E_C, is defined as the energy at which the cross-section for ionisation and bremsstrahlung are equal. This can be parameterised as a function of the atomic number of the absorber by $E_C \cong (800\ \text{MeV})/(Z+1.2)$.
- The radiation length X_0 is defined as the distance in the absorber normalised to its density over which a high-energy electron loses, on average 63.2% (1-1/e) of its energy by bremsstrahlung only. The radiation length can be parameterised within a 5% accuracy as $X_0 = 716.4A/[Z(Z+1)\ln(287/\sqrt{Z})]\ \text{g}\cdot\text{cm}^{-2}$ where Z is the atomic number and A the atomic weight. This can be well approximated by $X_0 \approx 180\ A/Z\ \text{g}\cdot\text{cm}^{-2}$ for $Z \geq 10$.

More and more particles are produced by radiation and pair production generating a shower but the average energy of these particles decreases as the shower continues. When the average energy of the shower particles reaches E_C the number of particles is at its maximum and further multiplication stops. The simple one-dimensional model can be used to predict that the depth of e.m. showers scales logarithmically with the initial particle energy E_0. Assume that in the shower of figure 2.3, each bifurcation results in an even splitting of the initial particle energy amongst the two final ones. By proceeding in this way, after t radiation

lengths, there will be 2^t particles. Neglecting ionisation loss and the energy dependence of radiation and pair-production cross sections, the energy per particle at depth t will be $E(t)=E_o/2^t$. This process continues until $E(t)=E_C$, when ionisation energy loss suddenly becomes important and no further radiation is possible. The shower will thus reach a maximum and then cease abruptly. The maximum will occur at $t=\ln(E_o/E_C)/\ln 2$.

The longitudinal development of the shower can be described in an almost material independent way in terms of the radiation length X_0, for high-energy showers. This scaling in X_0 is rather well confirmed by observations (see figure 2.4).

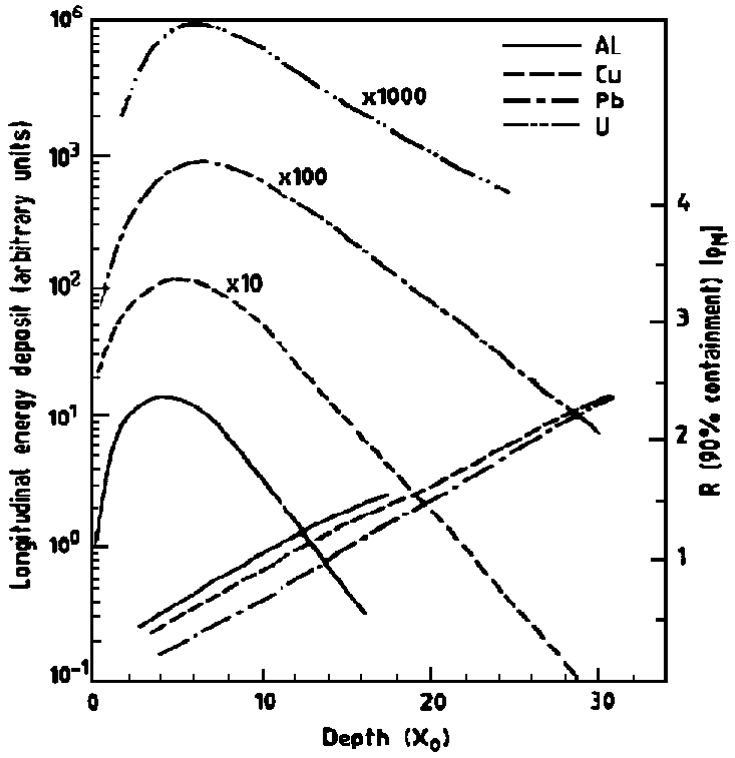

Figure 2.4. Longitudinal shower development (left ordinate) of 6 GeV/c electrons in three very different materials, showing the scaling in units of radiation lengths X_0. On the right ordinate the shower radius for 90% containment of the shower is given as a function of the shower depth.

A more complete analytical description of the longitudinal shower profile has been given by Rossi [2.3.] based on the following assumptions:

(a) the cross section for ionisation is energy independent, i.e. $dE/dx = -E_C/X_0$;
(b) multiple scattering is neglected and the e.m. cascade is treated one-dimensionally;
(c) Compton scattering is neglected.

A convenient analytical description of the profile can be given in the form:

$$\frac{dE}{dt} = E_0 b \frac{(bt)^{a-1} e^{-bt}}{\Gamma(a)} \qquad \text{(Eq. 2.1.)}$$

where $t = x/X_0$, and a and b are parameters such that t_{max} occurs at (a-1)/b .

The transverse shower properties can also be easily understood qualitatively. In the early, most energetic part of the cascade, its lateral spread is characterised by both the typical angle for bremsstrahlung emission, $\theta_{brems} \sim p_e/m_e$, and by the multiple scattering angle of electrons and positrons in the absorber. This later process increasingly influences the lateral spread as the average particle energy decreases and causes a gradual widening of the shower. In the later development of the cascade, the radial shower dimension scales with the Molière radius ρ_M (which describes the average lateral deflection of electrons of energy ε after traversing one radiation length). For the purpose of total energy measurement, the e.m. cascade occupies a cylinder of radius $R \cong 2\rho_M$, where $\rho_M = 21X_0/\varepsilon \cong 7A/Z$ [g cm^{-2}]. Typically an infinite cylinder of radius R contains 95% of the initial particle energy.

2.3. Experimental requirements and limitations for electromagnetic calorimetry

The main goal of calorimeters is energy measurement, but often position and angle measurements are also performed with them, as well as a certain degree of particle identification.

2.3.1 Energy measurement

The most important aspects of energy measurement are linearity and resolution. Non-linear response could be a major concern in experiments where particle energies cover a large range. For instance, in an LHC experiment, one has to measure electrons with a transverse energy from a few GeV ($H \rightarrow e^{\pm}$) up to a few TeV ($Z' \rightarrow e^+e^-$). Non-linearity is often due to the electronics chain and can in principle be corrected offline. Operating in a high magnetic field can also be a source of poor linearity at low energy.

The energy resolution gives the uncertainty in a calorimeter measurement and is usually parameterized by the following quadratic sum:

$$\frac{\sigma}{E} = \frac{a}{\sqrt{E}} \oplus \frac{b}{E} \oplus c \qquad \text{(Eq. 2.2.)}$$

where a is the stochastic term (intrinsic resolution), b the noise term, c the constant term and E is expressed in GeV. Depending on the energy range involved in an experiment, the optimisation of these three parameters can be very different.

The best resolution is commonly reached by thick homogeneous calorimeters. There the intrinsic resolution is given by the statistical fluctuation of the number of detected primary processes. The threshold of detection is usually small enough that the number of processes, which give a useful signal, is large and gives good intrinsic resolution. In general this fluctuations have to be convoluted with instrumental effects which dominate the resolution: uncertainty in the calibration, stability of the electronics, fluctuations in showers leakage, etc.

In a typical sampling calorimeter, the main contribution to the energy resolution is due to sampling fluctuations. The signal is only produced in the active layers and is therefore determined by the number of charged tracks crossing these layers. The total track length (T) is proportional to the incident particle energy but the number of tracks intercepted in the gap is only $N = f_{samp}\, T$. Then the energy resolution is given by the fluctuation in the number of tracks N:

$$\frac{\sigma(E)}{E} = \frac{1}{\sqrt{N}} \propto \frac{1}{\sqrt{f_{samp}} \cdot \sqrt{E(GeV)}} \qquad \text{(Eq. 2.3.)}$$

The approximation used is enough to demonstrate the energy dependence of the resolution. As a very large fraction of the energy is deposited by low-energy electrons (MeV) in the high-Z material (absorber), the energy resolution is improved when decreasing the absorber thickness (f_{samp} will be larger for smaller thickness). This scaling law is valid as long as the absorber thickness is not so small that the crossing between consecutive layers are not correlated.

The (b) term of the energy resolution describes the noise and is dominant at low energy. Besides the electronics noise, a second contribution is important in LHC calorimeters: the pile-up noise. At the LHC design luminosity, about twenty soft collisions will be produced, on average, every bunch crossing, giving rise to so-called pile-up both in space and time. This reflects the high multiplicity of charged and neutral particles with a low average momentum (500 MeV/c) which impact in the calorimeter during each bunch crossing. The fluctuations in the mean value of this pile-up contribute as a noise term to the energy resolution.

The constant term (c), dominant at high energy, includes many contributions:

- Non-uniformity of the calorimeter from both electronic and mechanical design.
- Signal variation with temperature or pollution of the active medium which may vary across the calorimeter or as a function of time.
- Lateral and longitudinal leakage.
- Degradation of the energy resolution due to the material in front of the calorimeter.

2.3.2 Position and angular measurement

The segmentation of calorimeters in strips or towers, which are read by different readout elements, has been used to find shower impact positions using centre-of-gravity methods. Practical detectors can reach resolutions at the level of a few mm/$\sqrt{E}$. The energy dependence come directly from the energy resolution in each of the cells.

The need for an angular measurement provided by the calorimeter has been stressed recently in the context of the $H \rightarrow \gamma\gamma$ channel produced in pp collision at the LHC. The $\gamma\gamma$ angle enters into the mass resolution, and since at high luminosity the vertex will not be known very precisely, it is necessary to measure this angle with the calorimeter. Such a measurement requires at least two segments in depth and a sufficiently long lever arm.

2.3.3 Particle identification

Rough particle identification is performed using as a basis the lateral and longitudinal shower profiles and comparing them to those expected from e.m. versus hadronic shower. The demands are quite different depending on the desired physics process.

2.4. Hadronic showers

When a hadron passes through matter, it interacts with the nuclei of the medium through strong interaction processes. This opens up a variety of possible ways for hadronic showers to develop, making them more difficult to describe and predict than e.m. showers. Basically, when a hadron enters the absorber, it interacts with a nucleus in such a way as to produce many secondary particles. These particles then lose their energy either by starting further reactions and creating more particles or by ionising the surrounding media, propagating a shower (Figure 2.5.) until all the incident energy is spent.

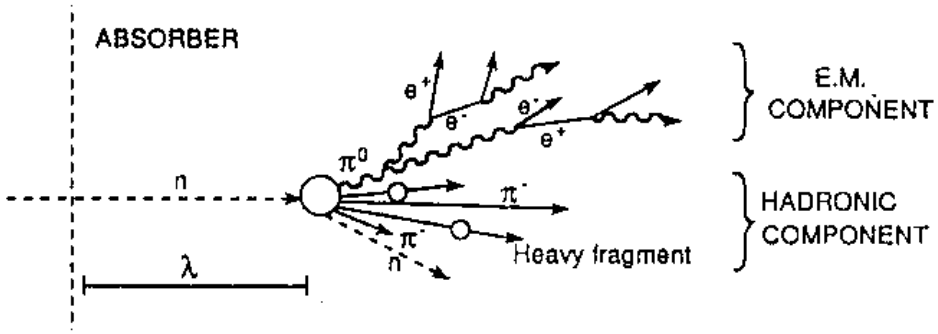

Figure 2.5. Hadronic shower development

Two main parts of a hadronic shower can be distinguished:

- A considerable part of the secondaries are π^0's, which will propagate electron-magnetically after the $\pi^0 \rightarrow \gamma\gamma$ decay without any further nuclear interactions (e.m. component). The size of the π^0 component is largely determined by the production of π^0 in the early stages of the shower development, and event by event fluctuations about the range values are therefore important.
- The rest of the hadron secondaries loose some energy by dE/dx in the material, but a sizeable amount of the available energy is converted into excitations or break-up of the nuclei. Therefore only a fraction of the energy loses will result in detectable ('visible') energy.

The distribution of the deposited hadron energy is similar to that of an e.m. shower in shape, but its dimensions scale roughly with the nuclear interaction length λ. A rough estimate can be made using:

$$\lambda\left[g/cm^2\right] \approx 35A^{1/3} \qquad \text{(Eq. 2.4.)}$$

The nuclear interaction length governs both the lateral and longitudinal dimensions of the hadronic shower.

The longitudinal shower maximum occurs at a distance from the front of the detector, t_{max} which may be parametrized by:

$$t_{\max}\left[\lambda\right] \approx 0.2 \cdot LnE + 0.7 \qquad \text{(Eq. 2.5.)}$$

where E is the energy of the incoming hadron in GeV. The depth required to contain on average 95% of the energy is:

$$t_{95\%}[\lambda] \approx t_{\max} + 2.5 \cdot E^{0.13} \qquad \text{(Eq. 2.6.)}$$

with t_{max} in units of λ and E in GeV. An experimental measurement of the longitudinal profile in a calorimeter is shown in Figure 2.6.

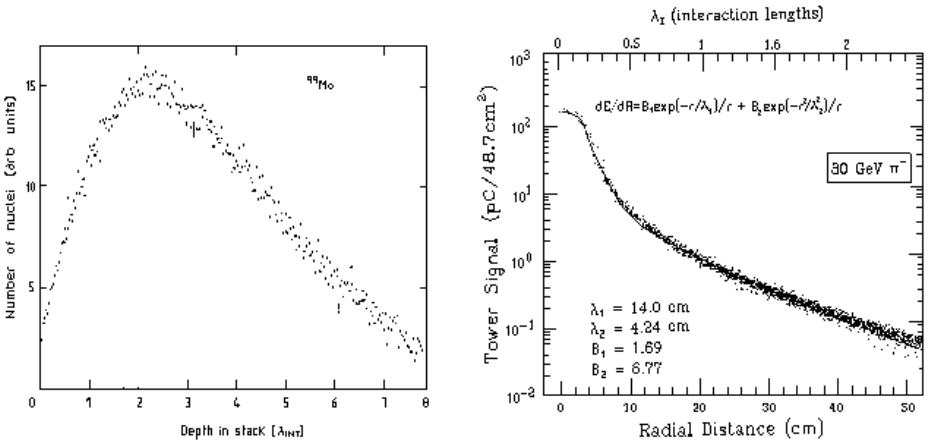

Figure 2.6. Longitudinal (300 GeV) and lateral hadronic shower profiles.

The lateral energy deposit profile shows a highly energetic, relatively collimated core due to π^0 production in the shower, with a halo produced by shower particles of lower energy which move further away from the shower axis. The lateral dimensions scale with λ, but also depend on the energy of the incident particle.

The shower dimensions can be used to distinguish between hadronic and e.m. showers most easily in materials with large Z. In this case, the ratio λ/X_0 is high and the hadronic showers are much longer and wider than the e.m. showers.

2.5. Energy resolution and limitations in hadronic calorimeters

As for e.m. calorimeters, one can parameterise the resolution by the relation defined in section 2.3.1. The first term, a, is the quadratic sum of sampling fluctuations and intrinsic resolution. The sampling fluctuations are roughly twice as large for hadronic showers than for e.m. showers in the same calorimeter. However, the sampling contribution is small and the dominant one is the intrinsic resolution. The fluctuations in hadronic shower development are greater than those for an e.m. shower. This is not only because the shower is produced by relatively few interactions, but also because processes develop very differently. There are large, non-Gaussian fluctuations in the e.m. fraction of hadron shower (f.e.m.), largely dependent on the nuclear interactions early in the shower. The fraction of energy that does not

produce a signal varies from event to event with an average of ~40%. These fluctuations contribute to the resolution in a statistical way, proportional to $E^{-1/2}$.

One of the most important parameters for energy resolution in a hadronic calorimeter is the ratio of observed signal for the e.m. and non e.m. components of a hadronic shower, the so-called e/h ratio. The consequences of $e/h \neq 1$ include:

- A contribution to the energy resolution due to fluctuations in $f_{e.m.}$;
- A non-linear response with energy;
- A non-Gaussian signal distribution;
- Deviations from scaling with $E^{-1/2}$, which dominate the energy resolution at high energies;
- Energy dependence of the measured e/π signal ratio.

Therefore, a compensating calorimeter is desirable for high-precision hadron detection. Various possibilities to achieve $e/h \sim 1$ have been investigated:

- The non-e.m. response can be increased by using a fissionable material as an absorber, such as depleted uranium. The extra energy created in the nuclear fission reaction can be detected in the readout material.
- The e.m. response can be decreased by combining a low-Z active material with a high Z-absorber in order to suppress the response from photoelectric effect in the active material.
- The non-e.m. response can be increased by using an hydrogenous material as the active component. In such a material, the cross effective section for elastic neutron scattering enlarge, with the energy released in this process going toward producing a signal.

The second term in the energy resolution parameterisation, b, as well as the constant term, c, has the same contributions than the ones for the e.m. calorimeter, i.e. electronic noise and pile-up for the second term; and energy miscalibration, non-uniformities, leakage, etc. for the constant term.

The two LHC experiments have chosen hadronic calorimeters without compensation. The ATLAS central hadronic calorimeter is made of large scintillating tiles based on a sampling structure with interleaved steel absorber and scintillating plates read out by

wavelength shifting fibres. Although the e/π ratio for such a calorimeter is around 1.1-1.2, the introduction of depth segmentation permits the application of software connections that restore linearity, thereby fulfilling the requirements at a lower cost than a compensating calorimeter.

2.6. ATLAS calorimeters requirements

2.6.1 Electromagnetic calorimeter requirements

REQUIREMENT	MOTIVATION	CHANNEL
Rapidity coverage $\|\eta\|=5$	E_T^{miss}, good acceptance for jet tagging	$H \rightarrow \gamma\gamma$, $H \rightarrow 4e$
Electron reconstruction from 1-2 GeV up to 5 TeV	Increase b-tagging efficiency by 10 % Maximum set by Z´ and W´ decays	Semileptonic decays of the b quarks, $H \rightarrow 4e$ Z' and W' decays
Excellent energy resolution in the range 10-300 GeV	~1% mass resolution in mass region 90-180 GeV ⩾ sampling term of the energy resolution ~10%/√E, constant term <1%	$H \rightarrow \gamma\gamma$ $H \rightarrow 4e$
Thickness of 24 radiation lengths at $\eta=0$	Keep fluctuations of high-energy showers not fully contained to an acceptable level	
Dynamic range from 50 MeV to 3 TeV	From typical electronic noise to maximum energy deposited in a cell	
Energy-scale precision 0.1%	~200 MeV precision on the H mass	$H \rightarrow \gamma\gamma$
Linearity of response better than 0.5% in the energy range up to 300 GeV	To ensure optimal mass resolution	$H \rightarrow \gamma\gamma$, $H \rightarrow 4e$
Measurement of the shower direction in θ with a resolution of 50 mrad/√E	The photon direction must be measured accurately to maintain angular contribution below the energy resolution contribution	$H \rightarrow \gamma\gamma$
Excellent γ/jet separation	To suppres γ-jet backgronds	$H \rightarrow \gamma\gamma$
Excellent e/jet separation	Rate of e's with p_T>20 GeV is 5 orders smaller than the rate of QCD jets of same p_T	W, Z, heavy-flavour decays
Excellent τ/jet separation	To separate τ-jet from a QCD-jet	MSSM heaviest H decays to pairs of τ-leptons
Speed of response and noise	Pile-up minimisation requires fast detector response and electronics, minimisation of the electronic noise requires high granularity and high-performance of electronics	

High granularity	Particle identification, low noise, position measurement, speed of response and energy resolution require transverse granularity not coarser than $\Delta\eta\times\Delta\phi=0.03\times0.03$ over the rapidity region used for precision measurements.	
Bunch-crossing identification	Needed time resolution is a few ns at 1 GeV	

2.6.2 Hadronic calorimeter requirements

REQUIREMENT		MOTIVATION	CHANNEL
Rapidity coverage $\|\eta\|=5$		Efficient tagging of forward jets, good missing p_T resolution	
Granularity:	$\Delta\eta\times\Delta\phi=0.1\times0.1$ for $\|\eta\|<3$	Longitudinal segmentation driven by particle identification and better energy resolution via weigthing in a non-compensating calorimeter (3 samplings are adequate for these purposes)	W → jet-jet
	$\Delta\eta\times\Delta\phi=0.2\times0.2$ larger η		
Energy resolution		Jet energy resolution at different levels in different η regions $\frac{\Delta E}{E}=\frac{50\%}{\sqrt{E}}\oplus3\%$ for $\|\eta\|<3$ $\frac{\Delta E}{E}=\frac{100\%}{\sqrt{E}}\oplus10\%$ for $3<\|\eta\|<5$	
Energy linearity: jet energy scale linear within 2% up to a transvers energy of 4 TeV		Study of quark compositness	
Total thickness 10 interaction lengths (e.m. and hadron calorimeters)		For shower containment, both for energy resolution and for reducing the background in the muon chambers	
Noise		Electronic noise level relevant at low luminosity for the quality of low energy jet reconstruction. But due to the high number of channels the dominant effect comes from the e.m. calorimeter.	

3. THE TILE CALORIMETER FOR ATLAS

3.1. ATLAS: The overall detector concept

ATLAS is a general-purpose detector for high energy pp collisions, which is designed to exploit the discovery potential of the Large Hadron Collider (LHC) being built at CERN. The LHC offers a large range of physics opportunities, including investigation of mass at electroweak scale, searches for heavy W-like and Z-like bosons, for supersymmetric particles, and for compositeness of the fundamental fermions, studies of CP violation in B-decays, and detailed measurements of top quark properties.

The overall layout of the ATLAS detector is shown in Figure 3.1.

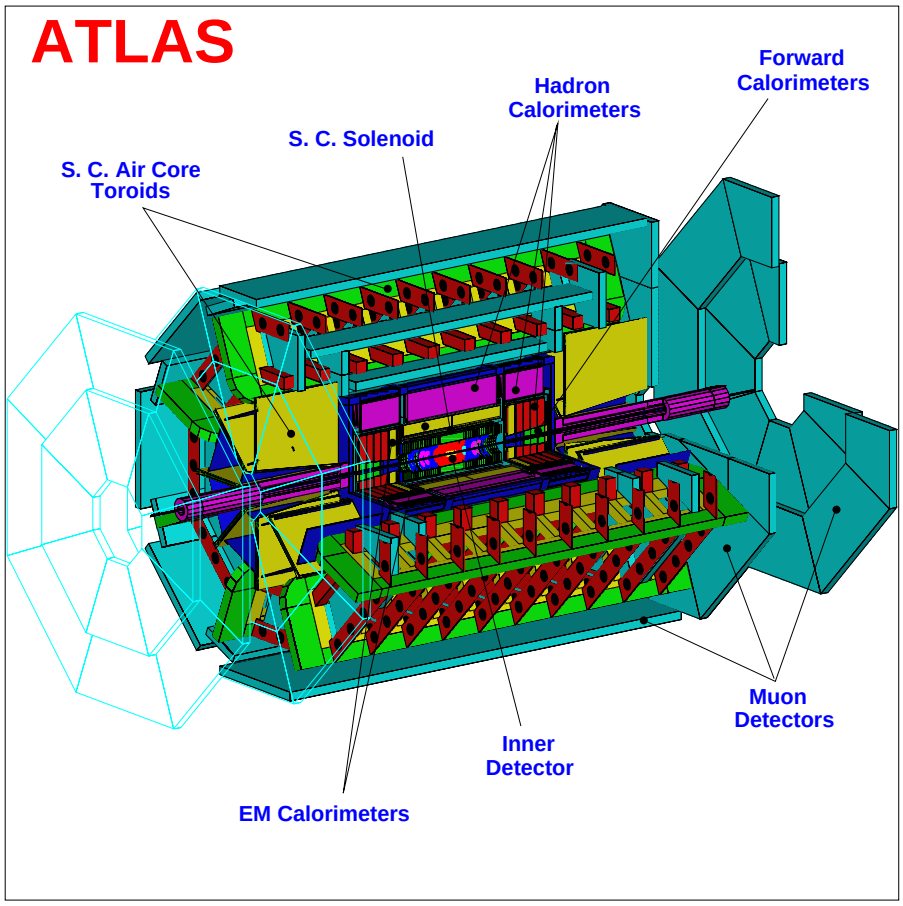

Figure 3.1. The ATLAS detector.

The magnet configuration is based on a inner superconducting solenoid around the inner detector cavity, and large superconducting air-core toroids consisting of independent coils arranged with an eight-fold symmetry outside the calorimetry. This concept offers:

- almost no constraints on calorimetry and inner detector allowing a wide choice of technological solutions;
- a high-resolution, large-acceptance and robust stand-alone muon spectrometer.

The inner detector is contained within a cylinder of length 6.80 m and radius 1.15 m, with a solenoidal magnetic field of 2 T. Pattern recognition, momentum and vertex measurements, and electron identification are achieved with a combination of discrete high resolution pixel and strip detectors in the inner part and continuous straw-tube tracking detectors with transition radiation capability in the outer part of the tracking volume.

A highly granular Liquid Argon (LAr) electromagnetic sampling calorimeter with excellent performance in terms of energy and position resolutions covers the pseudorapidity range $|\eta|<3.2$. In the end-caps the LAr technology is also used for the hadronic calorimeter, sharing the cryostats with the electromagnetic calorimeter end-caps. The same cryostats also house the LAr forward calorimeters which extend the η coverage to $3.2<|\eta|<4.9$. The bulk of the hadronic calorimetry is provided by a scintillator tile calorimeter of novel geometry, which is separated into one large barrel and two extended barrel cylinders on each side. The whole calorimeter system contributes to the very good jet and E_T^{miss} performance of the detector. A more detailed description of the calorimetry system can be found in the following section.

The calorimetry is surrounded by the muon spectrometer. Three stations of high precision tracking chambers with ~60 μm intrinsic resolution measure the coordinates of muons bending in the field. The muon instrumentation is complemented with fast trigger chambers.

The combination of all these subdetectors defines the overall dimensions of ATLAS. The outer chambers of the barrel are at a radius of about 11 m. The length of the barrel toroid coils is ±13 m, and the third layer of the forward muon chambers, mounted on the cavern wall, is located at ±21 m from the interaction point. The overall weight of the ATLAS detector is about 7000 tons.

3.2. The ATLAS Calorimetry

The tasks of the calorimeters at hadron colliders are: accurate measurement of the energy and position of electrons and photons; measurement of the energy and direction of jets, and of the missing transverse momentum of the event; particle identification, for instance separation

of electrons and photons from hadrons and jets, and of τ hadronic decays from jets; and event selection at the trigger level.

The above will also be the main tasks of the calorimeters at the LHC, made more difficult, however, by the parameters of the machine: high luminosity and the large centre-of-mass energy (14 TeV), which requires good performance over an unprecedented energy range, extending from a few GeV up to the TeV scale. At the LHC design luminosity (10^{34} $cm^{-2}s^{-1}$), about twenty soft collision will be produced, on average, every bunch crossing (i.e. every 25 ns), giving rise to so-called "pile-up" both in space and time. Fast detector response (<50 ns) and fine granularity are required to minimise the impact of the pile-up on the physics performance. High radiation resistance is also needed, given the high particle fluxes expected over a period of operation of at least ten years.

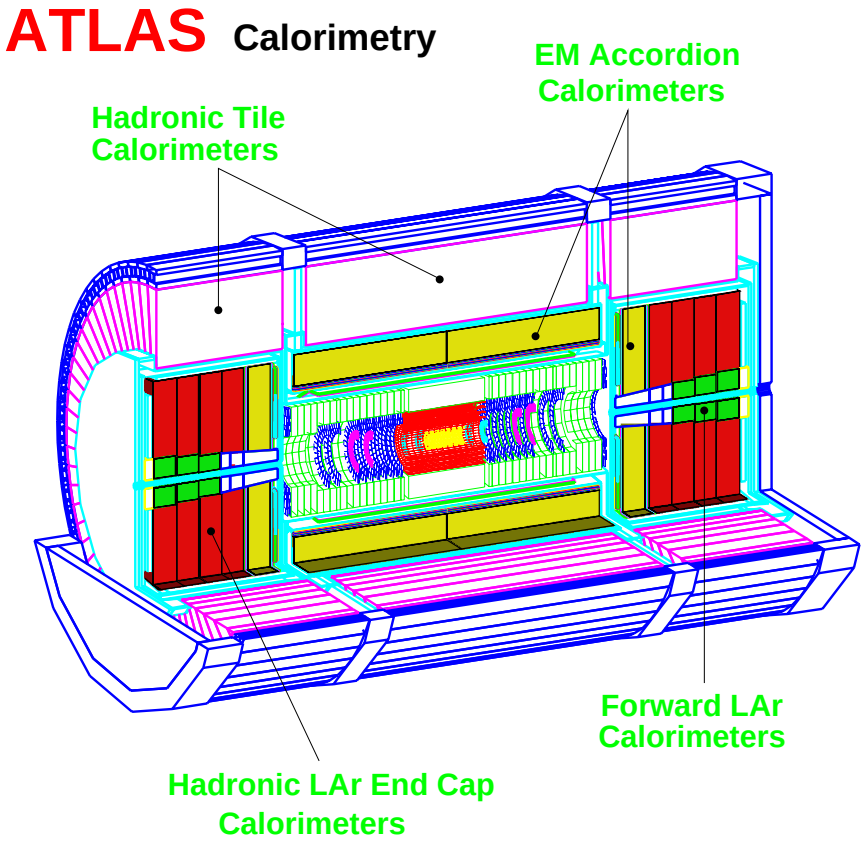

Figure 3.2. The ATLAS Calorimetry layout.

The ATLAS calorimeter has been designed to meet the diverse demands of the LHC physics program while operating in its very high luminosity environment. Figure 3.2 shows the calorimeter layout. A barrel cryostat around the inner detector cavity contains the barrel electromagnetic calorimeter and the solenoidal coil, which supplies a uniform magnetic field to the inner tracking volume. This coil is placed in front of the e.m. calorimeter. Two end-cap

cryostats enclose the electromagnetic and hadronic end-cap calorimeters as well as the integrated forward calorimeter. The barrel and the extended barrel hadronic calorimeters are contained in an outer support cylinder, acting also as the main solenoid flux return, and consist of scintillating tiles and iron absorber plates. The outer radius of the flux return behind TILECAL is 4.23 m. The length of each end-cap cryostat is 3.25 m.

3.3. The electromagnetic Calorimeter

Many important physics processes at the LHC, such as the decay of Higgs bosons into photons or electrons, or the detection of new gauge bosons (Z' or W') decaying to electrons, place stringent requirements on the e.m. calorimetry in terms of acceptance, dynamic range, particle identification, energy resolution, and direction measurement.

The e.m. calorimeter must be able to identify and accurately reconstruct electrons and photons over a wide energy range. The e.m. calorimeter uses lead absorbers in a liquid Argon ionisation calorimeter and it is divided into a barrel part ($|\eta|<1.475$) and two end caps ($1.375<|\eta|<3.2$) both implemented in an "accordion" geometry. The longitudinal and transverse segmentation of the electromagnetic calorimeter allows an estimation of the shower shape and is therefore an essential tool in rejecting jet backgrounds. The segmentation of the electromagnetic calorimeter has been chosen to be $\Delta\eta \times \Delta\phi \cong 0.025 \times 0.025$ over most of the rapidity coverage (ϕ is the azimutal angle in radians). The first sampling (4.5 X_0) has a much finer segmentation and therefore plays the role of a preshower device. The barrel part of the electromagnetic calorimeter is preceded by a presampler layer located immediately behind the cryostat inner wall. Measurement from the pre-sampler are used to correct for the energy lost in the material in front of the calorimeter (inner detector, coil, and cryostat) and to assist in measuring η for showers. The required resolution over the energy range of 10-300 GeV is a sampling term at the level of $10\%/\sqrt{E(GeV)}$ and a constant term that should be smaller than 1%.

3.4. The Hadronic Tile Calorimeter

TILECAL is the hadronic calorimeter of ATLAS and its technology is based on a sampling technique using steel absorber material and plastic scintillator plates read out by wavelength shifting (WLS) fibres. The unique feature of this hadron calorimeter is the orientation of the scintillating tiles relative to the direction of the particles from the interaction point. The tiles are placed in lanes perpendicular to the colliding beams and staggered in depth to provide a uniform sampling fraction.

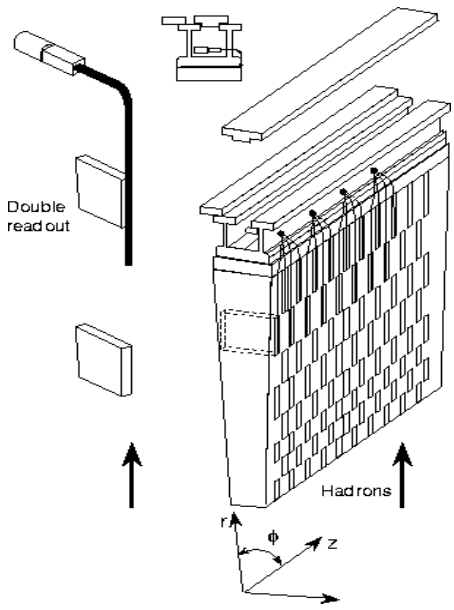

Figure 3.3. The principle to the Tile Calorimeter design.

3.4.1 The geometry of the Tile Calorimeter

The Tile Calorimeter consists of a cylindrical structure with inner and outer radius of 2280 and 4230 mm respectively. It is subdivided into a barrel part which is 5640 mm in length along the beam axis and two extended barrels which are 2910 mm long. Between the barrel and the extended barrels there is a gap of about 600 mm, which is needed for the Inner Detector and the LAr cables, electronics and services. The thickness of the calorimeter in the gap is improved by an Intermediate Tile Calorimeter (ITC), with the same structure as the rest of the calorimeter. The barrel covers the region $-1.0<\eta<1.0$, and the extended barrels cover the region $0.8<|\eta|<1.7$

Each detector cylinder is built of 64 independent modules along the azimutal direction. The highly periodic structure of the system allows the construction of these azimutal wedges by assembling smaller sub-modules together. Since the mechanical assembly is completely independent from the optical instrumentation, the design becomes simple and cost effective.

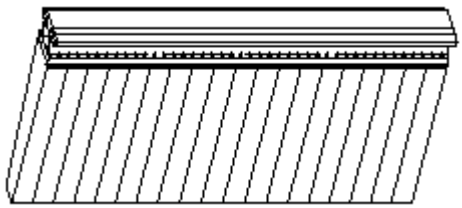

Figure 3.4. Schematic of Barrel Module.

The basic geometrical element, called a period (see figure 3.5), consists of two master plates (large trapezoids) 5 mm thick, and one set of spacer plates (small trapezoids) 4 mm in thickness. The spacer plates are placed between the master plates making two half periods. The relative position of the spacers in the two half periods is staggered in the radial direction to leave empty pockets where later on the 3 mm thick scintillator tiles are put (in the figure in black and grey).

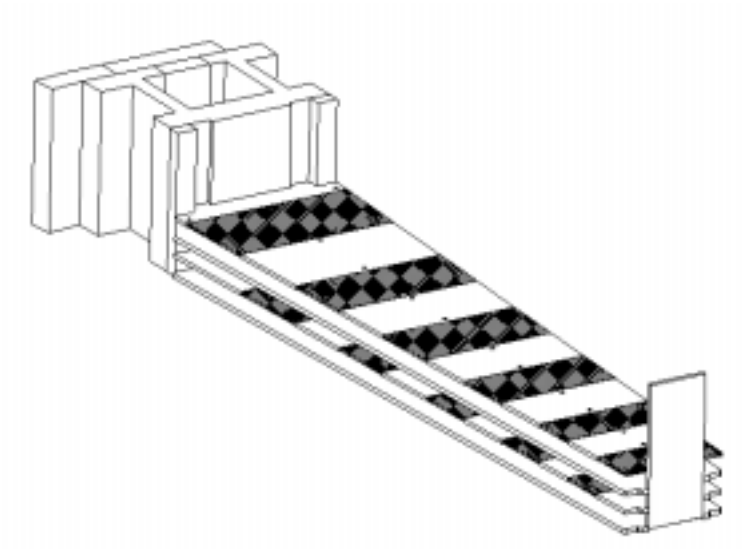

Figure 3.5. Exploded view of a period.

The thickness of the calorimeter (always at least 9λ) is chosen such that the hadronic showers are well contained and that there is enough material to reduce the particle flux reaching the muon system. In addition, the ability to identify muons will help to recover the momentum resolution for low energy muons where energy loss in the material tends to dominate.

3.4.2 The optics of the Tile Calorimeter

Eleven sets of tiles of radial sizes from 97 mm to 187 mm, pointing radially to the beam line, form the longitudinal segmentation of the detector. A pair of wavelength shifting (WLS) fibres running radially collects light from the tiles at both of their ϕ edges. Readout cells are defined by grouping together a set of fibres onto a PMT, to obtain three-dimensional segmentation. The $\Delta\eta \times \Delta\phi$ segmentation formed by the module geometry and scintillator cell structures is 0.1×0.1. In the last radial layer, where hadronic showers will be broad, the segmentation is 0.2×0.1. And the radial segmentation at $\eta=0$ corresponds to approximately 1.4, 4.0 and 1.8 λ.

Ionising particles crossing the tiles induce the production of light in the base material of the tiles, with wavelengths in the UV range, which subsequently is converted to visible light by scintillator dyes. This scintillation light propagates through the tile to its edges, where it is absorbed by the WLS fibres and shifted to a longer wavelength (chosen to match the sensitive region of the PMT photocathode). A light mixer is placed between the fibres and the photocathode to optimise detection uniformity

The driving philosophy behind the optics is to achieve and maintain a uniform, minimum light yield that achieves the required resolution. The necessary photostatistics corresponds to a photoelectron yield of 0.5, which could increase up to 1 by adding a safety factor, photoelectrons per minimum ionising particle (mip) per tile at normal incidence. The photoelectron yield is a complex factor depending not only on the light output of the tiles, but also on the light collection efficiency, the PMT choice and the fibre choice.

Non-uniformity throughout the detector should also be kept small so as not to impact the constant term of the resolution. The baseline goal is an rms non-uniformity within a cell up to 10%. The radial signal variations inside a cell due to the fact that more than one tile is read by the same fibre are of the order of 5% and cannot be improved without substantially increasing the number of fibres. So, to realise an overall non-uniformity of 10% rms, it will be necessary to keep non-uniformity inside a tile, tile-to-tile fluctuations, and fibre-to-fibre fluctuations below 5%.

Furthermore, the detector is expected to operate a minimum of 10 years. Typical ageing rates for a scintillator-WLS system is 1-3% loss of light per year. To provide a safety margin for ageing and other effects a requirement of a minimum light yield > 1.2 pe/mip/tile at production was set.

The Scintillator System

The scintillating tiles are the active medium of TILECAL. Light yield, uniformity of response within a tile and tile-to-tile uniformity are key performance issues. Each of the calorimeter sections will be equipped with tiles of the same dimension.

TILECAL contains 11 different sizes of trapezoidal shaped tiles, ranging from about 200 to 400 mm in ϕ length and from 97 to 187 mm in radial width. The WLS fibres are placed in contact with the non-parallel edges of the tiles. The tile thickness is 3 mm. Each tile has two

holes, 9 mm in diameter, through the surface for the passage of the calibration source tubes, which also serve as a mechanical fastener.

Commercially available optically transparent granulated polystyrene is used as the scintillation matrix base. The polystyrene is dried and then mixed with finely dispersed wavelength shifting dyes. The wavelength shifting process consists of a sequence of light absorptions and emissions in the chosen dye system. The dopants chosen were paraterphenyl (PTP) -1.5%- and POPOP -0.04%-. In a binary scintillator such as used in TILECAL, the initial radiation at the wavelengths 240-300 nm induced by the ionising particle is transmitted through the polystyrene lattice until it is absorbed by a primary flour PTP molecule. PTP emits light in the range 320-400 nm, which is absorbed by POPOP and converted to a longer blue wavelength (around 420 nm and higher).

The uniformity of the light output of a tile depends on the local light yield uniformity and on the tile transparency. Fluctuations in tile properties depend on both the raw material properties and the stability of the moulding machine operation. The existence of internal stresses, flow lines and other plastic deformations seen in the tiles may affect their optical quality.

Before the scintillating tiles are inserted into TILECAL, they are wrapped with a covering material. The wrapper protects the optically reflective surface of the tile from contact with materials having an index of refraction which would spoil the internal reflection of the light. It also provides protection from mechanical damage and, in addition, enhances the light yield by redirecting some of the light which is not captured by internal reflections back into the tile. To achieve a non-uniformity across the tiles below 5%, a non-reflective mask will be printed on the wrapper. Tyvek^{TM}, a material made of high density polyethylene fibres, has been chosen because of its high reflectance and toughness. The gain in light output is between 5 and 10%, compared to ordinary paper wrapping, and about 20% compared with unwrapped tiles.

The WLS fibres

Each fibre collects scintillation light from of one or two tiles and transmits it to a PMT in the girder. This is accomplished by the flour in the fibre which absorbs the blue light from the scintillator and re-emits it at a longer wavelength. The light subsequently propagates along the fibre by total internal reflection. Ideally, the light collection should be efficient, fast, with low attenuation along the fibre and the fibres should be radiation hard. WLS fibres of 1 mm in diameter have been chosen for the test modules.

Four fibres for the barrels and three for the extended barrels are required to read out one side of each half-period. In the barrel the fibre length ranges from between 85 cm and 210 cm, depending on which cell is to be read and the location of the half-period. In the extended barrel the fibre length ranges from 90 cm to 230 cm.

The WLS fibres have been selected to have the following requirements:

- the absorption spectrum of the fibre should match the emission spectrum of the scintillator and the emission spectrum of the fibre should match the quantum efficiency of the PMT,
- the fibres should have maximum light yield and attenuation length,
- the fibres should be flexible and suffer minimum damage by stress due to curved paths,
- the direct fibre response (Cherenkov and scintillation light) to ionising particles should be small in order to avoid large signals from particles passing between modules,
- they should be radiation hard, for a total dose of 400 Gy,
  natural ageing over ten years should be negligible.

Fibre routing

The TILECAL modules are pseudo-projective in η. The cell geometry for half of a barrel module is shown in Figure 3.6 and for a full extended barrel in Figure 3.7.

The light output of a cell depends on many parameters. One of the most important ones is the light budget, which is defined as the product of the tile response with the fibre response. The cells within TILECAL group several tile sizes and several fibre lengths, in general leading to non-uniformities of light output within a cell and amongst cells themselves. It is the purpose of the fibre routing design to minimise these non-uniformities. The conditions that should be satisfied by the fibre routing design are:

- non-uniformity within cells should be minimised,
- light output should be maximised in order to keep up the photostatistics level,
- fibre length should be minimal for optimum light output, to minimise the volume of the fibre in the girder region and also to minimise the cost,
- non-uniformity amongst cells should be small to allow PMTs to have similar gains,
- the number of different fibre lengths should be small for an efficient fibre insertion procedure.

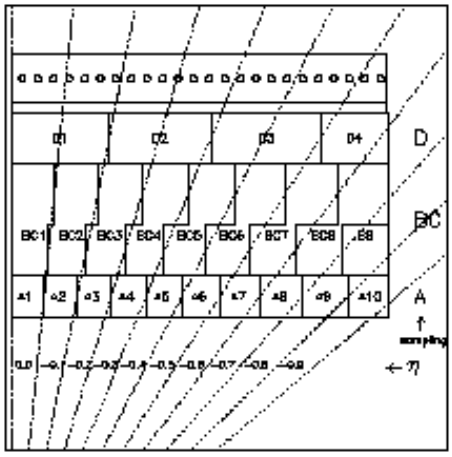

Figure 3.6. Cell geometry of half of a barrel module.